Available online at www.sciencedirect.com
ScienceDirect
Surface Science 600 (2006) 4888–4895
SURFACE SCIENCE
www.elsevier.com/locate/susc

Phosphine and tertiarybutylphosphine adsorption on the indium-rich InP (0 0 1)-(2 × 4) surface

R.L. Woo [a], U. Das [b], S.F. Cheng [a], G. Chen [a], K. Raghavachari [b], R.F. Hicks [a,*]

[a] Department of Chemical and Biomolecular Engineering, University of California, Los Angeles, CA 90095, United States
[b] Department of Chemistry, Indiana University, Bloomington, IN 47405, United States

Received 10 February 2006; accepted for publication 11 August 2006
Available online 1 September 2006

Abstract

Phosphine and tertiarybutylphosphine adsorption on the indium-rich InP (0 0 1)-(2 × 4) surface at 25 °C have been studied by internal reflection infrared spectroscopy, X-ray photoelectron spectroscopy, and low energy electron diffraction. Both molecules form a dative bond to the empty dangling bonds on the In–P heterodimers and the second-layer In–In dimers and vibrate symmetrically at 2319 (2315) and 2285 (2281) cm^{-1} and asymmetrically at 2339 (2339) and 2327 (2323) cm^{-1}. A fraction of these species dissociate into adsorbed PH_2 with the hydrogen and tertiarybutyl ligands transferring to nearby phosphorus sites. The calculated energy barriers for desorption (<11 kcal/mol) of these molecules is less than that for dissociation (>17 kcal/mol) and explains their low sticking probabilities at elevated temperatures under InP growth conditions.

Keywords: Indium phosphide (InP); Phosphine; Tertiarybutylphosphine; Infrared spectroscopy; Cluster calculations; Density functional theory

1. Introduction

Metalorganic chemical vapor deposition (MOCVD) is one of the essential technologies for manufacturing optoelectronic devices such as light emitting diodes, solid-state lasers, high efficiency multijunction solar cells, and heterojunction bipolar transistors [1–5]. The performance of these devices is affected in a major way by the deposition process. For example, the emission intensity of long wavelength InGaAsP/InP lasers depends highly on the interface abruptness during epitaxial growth [6]. The most important factors influencing this abruptness is the mass transport in the boundary layer coupled with the chemical reactions taking place on the film surface [6,7]. A better understanding of the heterogeneous reaction chemistry could lead to further improvements in the MOCVD process.

Phosphine (PH_3) and tertiarybutylphosphine (TBP) supply the group V sources to the semiconductor crystal during MOCVD growth [8–12]. Using in situ monitoring of the phosphorus coverage by reflectance difference spectroscopy (RDS), Sun et al. [13,14] measured the reaction kinetics of PH_3 and TBP with the InP (0 0 1) surface. They observed that the sticking probability of TBP decreases from 0.007 to 0.001 with increasing temperature from 420 to 520 °C; whereas the sticking probability of PH_3 is approximately equal to 0.001 over the same range. Based on the kinetic measurements, Sun proposed the following mechanism for the decomposition of the group V sources on indium phosphide (using TBP as an example):

$$^{*}_{In} + TBP(g) \leftrightarrow {}^{*}_{In}TBP \quad (1)$$

$$^{*}_{P} + {}^{*}_{In}TBP \rightarrow {}^{*}_{P}L + {}^{*}_{In}PL_2 \quad (2)$$

$$^{*}_{In}PL_2 \rightarrow {}^{*}_{P} + \text{products} \quad (3)$$

where L is an alkyl group or a hydrogen atom. Initially, the TBP molecule is believed to form a dative bond with the empty dangling orbital on an exposed indium atom. This

* Corresponding author. Tel.: +1 310 206 6865; fax: +1 310 206 4107.
E-mail addresses: kraghava@indiana.edu (K. Raghavachari), rhicks@ucla.edu (R.F. Hicks).

0039-6028/$ - see front matter © 2006 Elsevier B.V. All rights reserved.
doi:10.1016/j.susc.2006.08.014

reaction is reversible. Then, TBP undergoes dissociative adsorption and decomposes to form phosphorus dimers. Sun and coworkers did not explain why the sticking probability of the group V precursors is so low on InP (0 0 1). In addition, the datively bonded state has not been observed experimentally.

In this report, we present a study of phosphine and tertiarybutylphosphine adsorption on the indium-rich InP (0 0 1)-(2 × 4) surface. Using vibrational spectroscopy, we have identified the reaction intermediates, and have shown that the datively bonded molecule plays a significant role in the adsorption process.

2. Experimental and theoretical methods

An indium phosphide film, 35 nm thick, was grown on an InP (0 0 1) substrate by MOCVD. The following conditions were used during growth: 530 °C, 60 Torr of hydrogen, 6.7×10^{-4} Torr of trimethylindium (TMIn), 7.9×10^{-3} Torr of TBP (V/III ratio of 117), and a total flow rate of 33 L/min (at 25 °C and 760 Torr). Once the growth was completed, the TBP and the hydrogen flows were maintained until the sample was cooled down to 300 and 24 °C, respectively. Then, the sample was transferred to an ultrahigh vacuum chamber without air exposure. In vacuum, the sample was annealed at 500 °C for 15 min to obtain the (2 × 4) reconstruction.

After cooling the samples to 25 °C, the surface structure and composition were characterized by low energy electron diffraction (LEED) and X-ray photoelectron spectroscopy (XPS). Core level photoemission spectra of the P 2p and In 3d lines were collected with a PHI 3057 spectrometer using magnesium K_α X-rays ($h\nu = 1286.6$ eV). All XPS spectra were taken in small area mode with a 7° acceptance angle and 23.5 eV pass energy. The detection angle with respect to the surface normal was 25°. The P and In atom% were determined from the integrated intensity of the P 2p and In 3d photoemission peaks, dividing by their sensitivity factors, 0.49 and 4.36, respectively. The P/In ratio was obtained by dividing the P atom% by the In atom%.

The infrared spectra were recorded by multiple internal reflections through a trapezoidal InP crystal, $40.0 \times 10.0 \times 0.64$ mm^3. The long crystal axis was parallel to the [1 1 0] direction. This crystal provided for 31 reflections off the front face, which significantly enhanced the signal-to-noise ratio. The group V molecules were introduced into the UHV chamber at 5.0×10^{-6} Torr through a leak valve. Dosing was continued for up to 45 min to ensure that the InP (0 0 1)-(2 × 4) surface was completely saturated with TBP or PH_3. A series of infrared spectra was collected before and during TBP and PH_3 adsorption. These spectra were recorded by taking 1024 scans at 8 cm^{-1} resolution. The spectra presented in this paper show the change in reflectance (per reflection) that results from taking the ratio of the sample spectrum after dosing to that of the clean surface. During these experiments, all of the filaments in the chamber were turned off in order to avoid exposing the surface to dissociated radicals.

The calculations were performed using density functional theory (DFT) with the Becke three-parameter exchange functional and the Lee–Yang–Parr correlation functional (B3LYP). We chose the (18s/14p/9d)/[6s/5p/3d] contracted basis set for indium, the Dunning–Huzinaga (11s/7p/1d)/[6s/4p/1d] contracted basis set (D95**) for phosphorus, the D95** polarized double-ζ basis set for the surface hydrogen atoms and the D95 double-ζ basis set for the terminating hydrogen atoms. In previous work on hydrogen adsorption on P-rich indium phosphide surface, Fu et al. have successfully applied a single frequency shift for each mode to map the calculated vibrational frequencies onto those observed by experiment [15]. We have used the same approach here: the predicted P–H stretching frequencies have been uniformly shifted down by 110 cm^{-1} to correct for systematic errors in the calculations due to deficiencies in the cluster models, neglect of anharmonicity, and so forth.

3. Results

3.1. Phosphine adsorption

Shown in Table 1 are the atomic percentages of indium and phosphorous measured by XPS on the clean and covered InP (0 0 1) surfaces. Since the InP (0 0 1)-(2 × 1) and InP (0 0 1)-δ(2 × 4) surfaces have known phosphorus coverages of 1.00 and 0.125 [16], we used the atomic % of In and P on the clean surfaces to estimate the coverages on those dosed with PH_3 and TBP. Phosphine adsorption onto the InP (0 0 1)-(2 × 4) surface at 25 °C caused the P/In ratio measured by XPS to increase from 0.85 to 1.20. This suggests that the surface contains over 2.0 monolayers of adsorbed phosphorus. At the same time, the (2 × 4) LEED pattern gradually converted to a (1 × 1), indicating that the phosphine molecules reacted with the exposed In–P and In–In dimers and disrupted the local ordering.

Shown in Fig. 1 are a series of infrared reflectance spectra for different phosphine dosages on the (2 × 4) at 25 °C (1 L = 1×10^{-6} Torr s). In these spectra, there is a set of sharp peaks between 2350 and 2200 cm^{-1} and several broad bands between 1750 and 1000 cm^{-1}. The higher frequency peaks are due to P–H stretching modes, while the

Table 1
The percentages of In and P atoms observed by XPS on the clean, PH_3 and TBP covered InP surfaces

Surface	In %	P %	P/In	θ_p (ML)[a]
InP (0 0 1)-(2 × 1)	49.9	50.2	1.00	1.00
InP (0 0 1)-(2 × 4)	54.0	46.0	0.85	0.13
PH_3: InP (0 0 1)-(2 × 4) @ 25 °C	45.3	54.7	1.20	2.20
TBP: InP (0 0 1)-(2 × 4) @ 25 °C	48.7	51.3	1.05	1.30
PH_3: InP (0 0 1)-(2 × 4) @ 180 °C	50.0	50.0	1.00	1.00
PH_3: InP (0 0 1)-(2 × 4) @ 270 °C	55.1	44.9	0.81	0.13

[a] Based on linear extrapolation.

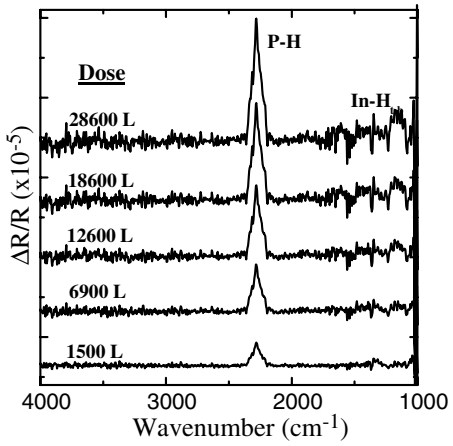

Fig. 1. Infrared reflectance spectra of adsorbed phosphine on InP (0 0 1)-(2 × 4) at 24 °C and different phosphine dosages.

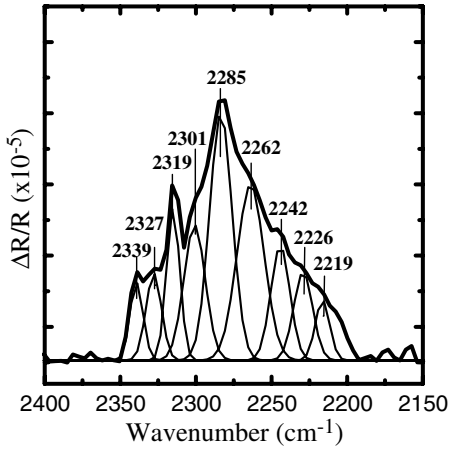

Fig. 2. Infrared reflectance spectra of adsorbed phosphine on InP (0 0 1)-(2 × 4) showing the deconvolution of the bands.

bands at lower frequency result from indium hydrides [15–19]. The intensity of the In–H vibrational modes is small compared to the P–H peaks. Shown in Fig. 2 is the deconvoluted infrared spectrum of the phosphorus–hydrogen stretching modes at saturation coverage. Nine overlapping peaks are observed at 2339, 2327, 2319, 2301, 2285, 2262, 2242, 2226, and 2219 cm^{-1}. The full-width-at-half maximum (FWHM) of these bands varies from 9.0 to 18.0 cm^{-1}.

Phosphine adsorption experiments were also performed at 180 and 270 °C. In the former case, the (2 × 4) LEED pattern gradually converted to a weak (1 × 2) whereas in the latter case, the (2 × 4) pattern remained but the spot intensity became weaker. The P/In ratio calculated from the XPS spectra was 1.00 and 0.81 at 180 and 270 °C, respectively. As shown in Table 1, these P/In ratios indicate that the phosphorus coverage is 1.00 ML at 180 °C and 0.13 ML at 270 °C. Evidently, phosphine does not stick to the surface at 270 °C and a PH_3 partial pressure of 5.0×10^{-6} Torr.

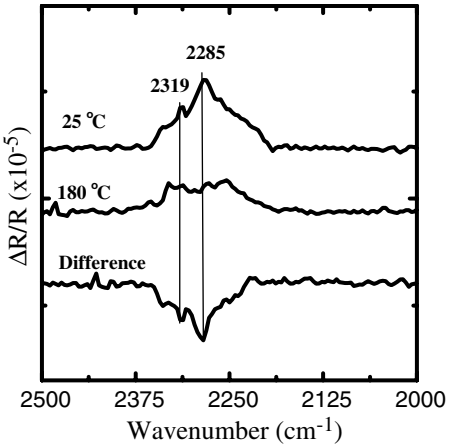

Fig. 3. Infrared reflectance spectra of adsorbed phosphine on the InP (0 0 1)-(2 × 4) surface at different temperatures.

Presented in Fig. 3 are infrared reflectance spectra taken after dosing 20,000 L of phosphine at 25 and 180 °C, and their difference in peak intensity. Note that larger dosages do not change the spectra. Inspection of the figure reveals that the intensities of the P–H bands are reduced at elevated temperature. Among these, the peaks at 2319 and 2285 cm^{-1} have decreased by the largest amount, indicating that the adsorbed species corresponding to these peaks are the most sensitive to changes in temperature. No absorption bands were observed at 270 °C as expected.

3.2. Tertiarybutylphosphine adsorption

Upon dosing indium phosphide with 25,000 L tertiarybutylphosphine at 24 °C, the (2 × 4) reconstruction was replaced by the (1 × 1), and the P/In ratio obtained from the XPS spectra increased from 0.85 to 1.05. The latter P/In ratio yields an estimated phosphorus coverage of 1.3 ML. Shown in Fig. 4 are a series of infrared spectra taken at different dosages of TBP at room temperature. In these spectra, there are five main sets of bands appearing

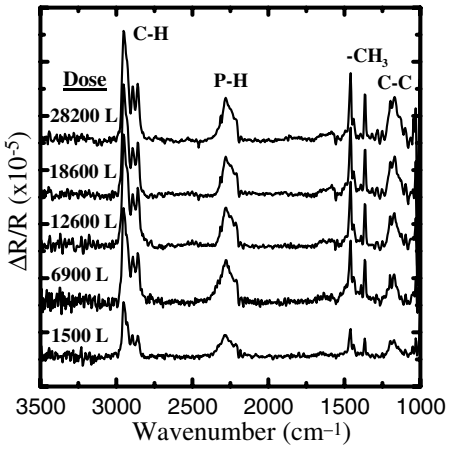

Fig. 4. Infrared reflectance spectra of adsorbed tertiarybutylphosphine on InP (0 0 1)-(2 × 4) at 24 °C and different TBP dosages.

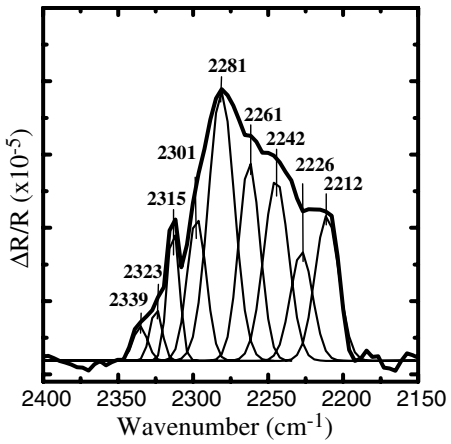

Fig. 5. Infrared reflectance spectra of adsorbed tertiarybutylphosphine on InP (0 0 1)-(2 × 4) showing the deconvolution of the bands.

in the following frequency ranges: 3000 to 2800 cm^{-1}, 2350 to 2200 cm^{-1}, 1480 to 1435 cm^{-1}, 1385 to 1350 cm^{-1}, and 1230 to 1000 cm^{-1}. The peaks in the frequency range between 2350 and 2200 cm^{-1} are due to P–H stretching modes [15–19]. The bands between 3000 and 2800 cm^{-1} result from CH_3 stretching modes, while those between 1480 and 1435 cm^{-1}, and 1385 and 1350 cm^{-1} are due to CH_3 bending modes [20–22]. Finally, the peaks between 1230 and 1000 cm^{-1} are assigned to C–C skeletal vibrations.

Shown in Fig. 5 is the deconvoluted infrared spectrum of the P–H stretching modes obtained at saturation coverage. Individual peaks are observed at 2339, 2323, 2315, 2301, 2281, 2261, 2242, 2226, and 2212 cm^{-1}. Their FWHM varies from 7.0 to 16.0 cm^{-1}. The number of peaks seen for TBP adsorption is the same as that seen for PH_3 adsorption (refer to Fig. 2). Moreover, the position and relative intensities of the peaks recorded for TBP are only slightly different from those seen for PH_3.

4. Discussion

4.1. Peak assignments

To interpret the vibrational spectra, we must understand the atomic structure of the (2 × 4) reconstruction. A filled-states scanning tunneling micrograph of the In-rich (2 × 4) surface is shown in Fig. 6 [16,17]. In this reconstruction, uniform gray rows extend along the [−1 1 0] direction, and the step edges lie straight along the rows. In the inset picture, a close up of the (2 × 4) unit cell is highlighted with a white rectangle. Within each cell, one can see three bright spots forming an equilateral triangle. These spots result from the filled phosphorus dangling bond and the two In–In back-bonds of each In–P dimer [17]. A ball-and-stick model of the (2 × 4) is presented in Fig. 6b. A single In–P heterodimer straddles four In dimers located in the next lower layer, with a phosphorus coverage of 0.125 monolayers (ML). In addition, each set of four indium dimers is separated by a trench that is parallel to the [−1 1 0] direction. In this reconstruction, the empty dangling bonds associated with indium on the In–P heterodimer and the second-layer In–In dimers are available for chemical bonding [16,24].

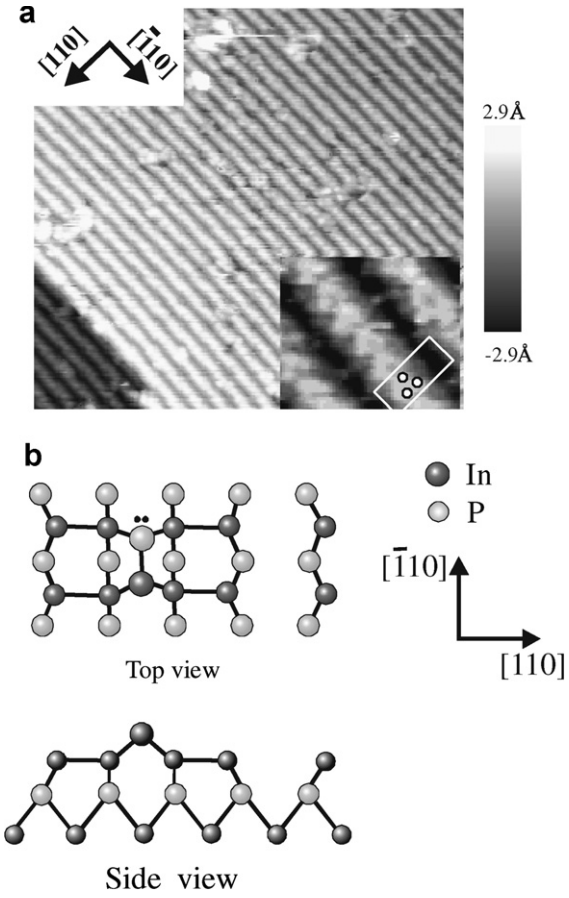

Fig. 6. (a) Filled-states STM image of the InP (0 0 1)-(2 × 4) reconstruction (440 × 440 $Å^2$; (inset) 40 × 40 $Å^2$) and (b) ball-and-stick model [16,17].

In order to assign the vibrational modes to specific bond configurations, molecular cluster calculations using the GAUSSIAN 03 quantum chemistry suite have been performed. To mimic the (2 × 4) reconstruction, cluster **1** was assembled as shown in Fig. 7. It contains one In–P mixed dimer connected to two indium dimers in the next layer. The two In–In dimers are tethered to eight "bulk" P atoms and three "bulk" In atoms. The cluster terminations have been carefully chosen to achieve a proper balance between covalent and dative bonding appropriate for compound semiconductors [18,26]. Note that cluster **1** represents roughly one half of the (2 × 4) unit cell and is of sufficient size to investigate the adsorption mechanisms of PH_3 and TBP.

To simulate phosphine adsorption on the indium-rich (2 × 4) reconstruction, phosphine was added to cluster **1**. Ab initio calculations were performed to determine the optimum configurations and the optimized molecular clusters, **2**, **3**, **4**, and **5**, are presented in Fig. 7. Cluster **2** reveals the initial stage of phosphine adsorption onto the empty In dangling bond in the heterodimer. In this case, a lone pair

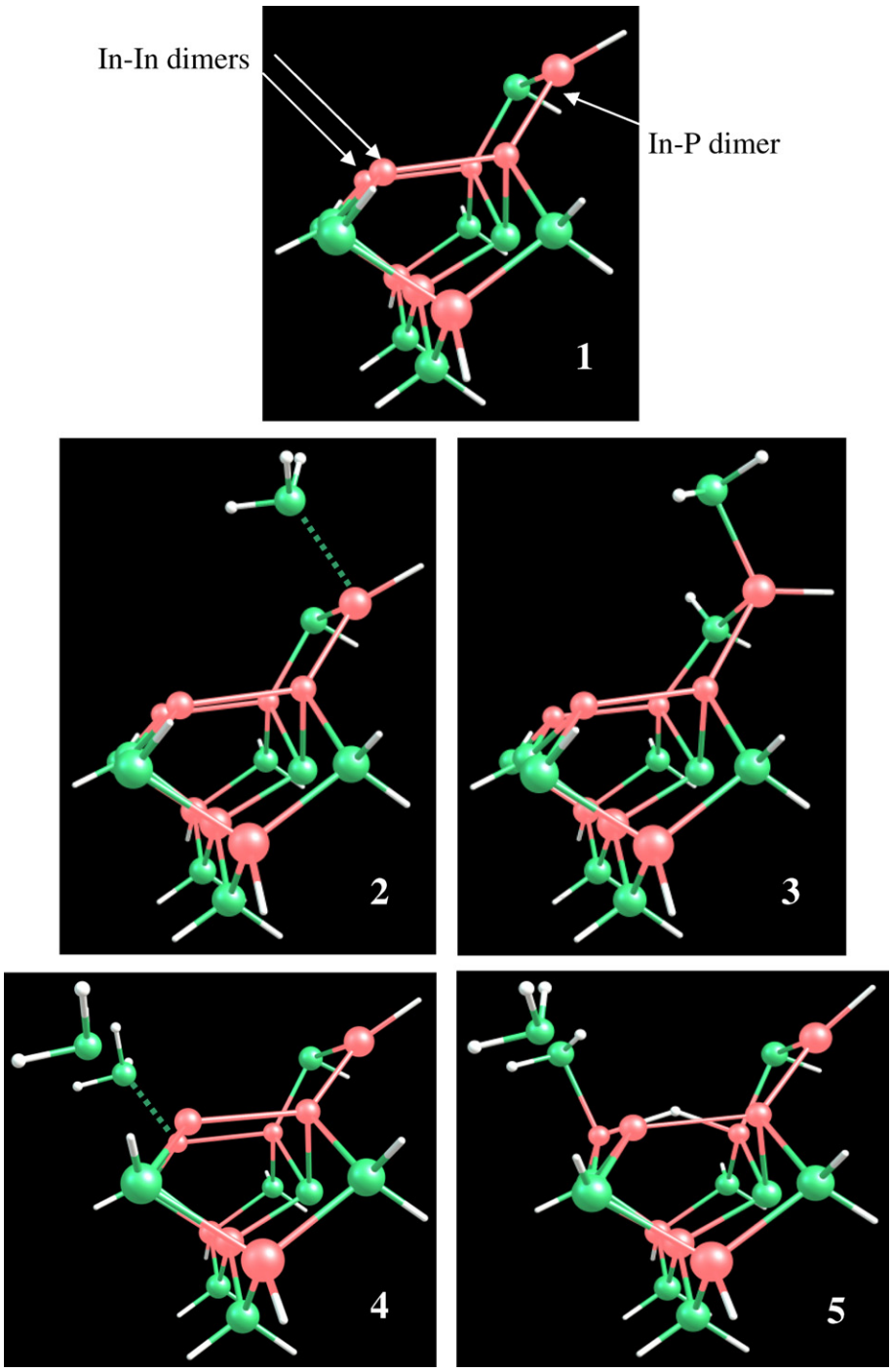

Fig. 7. Ball-and-stick models of the optimized clusters illustrating the different ways phosphine molecule coordinate to adsorption sites and surface species during dissociative adsorption of phosphine. The In, P, and H atoms are the large red, large green, and small white spheres, respectively.

of electrons from the phosphine molecule is donated to form a weak dative bond between phosphine and the indium atom. In cluster **3**, the phosphine molecule has dissociatively adsorbed onto the InP heterodimer, forming phosphorus dihydrogen and monohydrogen species. Note that the phosphorus atom associated with the PH_2 species contains a lone pair of electrons.

The phosphine molecules also may form dative bonds to the empty dangling bonds on the In–In dimers in the next layer. This is illustrated by cluster **4**. Two phosphine molecules are shown datively bonding to the indium atoms (second dashed line is omitted for ease of viewing). The datively bonded phosphine molecules in cluster **4** may dissociate into phosphorus dihydrogen species and transfer the hydrogen to the bridging position between the In dimer atoms. This configuration is illustrated in cluster **5** for one of the PH_3 molecules. The PH_2 species is covalently bonded to the indium atom and the P atom still retains

Table 2
Comparison of the P–H vibrational frequencies and relative intensities determined by experiment and theory

Assignments	Theory			Experiment			
				PH_3		TBP	
	ν	I	Model[a]	ν	I	ν	I
PH_3^s (In–P heterodimer)	2318	0.7	2	2319	0.7	2315	0.6
PH_3^{as}	2338	0.3	2	2339	0.2	2339	0.1
P–H	2319	0.4	3	2301	0.8	2301	0.7
PH_2^s	2245	0.7	3	2242	0.8	2242	0.9
PH_2^{as}	2255	0.8	3	2262	0.9	2261	0.9
PH_3^s (In–In dimer)	2296	1	4	2285	1	2281	1
PH_3^{as}	2329	0.2	4	2327	0.3	2323	0.2
PH_2^s	2233	0.8	5	2226	0.3	2226	0.5
PH_2^{as}	2242	0.7	5	2242	0.8	2242	0.9

ν = frequency (cm^{-1}).
I = relative intensity.
as = asymmetric, s = symmetric.
[a] Refer to Fig. 7.

its lone pair of electrons. The H atom is predicted to form a 3-center-2-electron bond with the In dimer atoms.

The P–H vibrational modes calculated for clusters **2** through **5** are listed in Table 2 along with the P–H vibrational modes observed in the experiments. Also shown in the Table is the relative intensity of each infrared band, which is defined as follows:

$$I = |I_{\nu(\mathrm{P-H})}|/|I^{\mathrm{Max}}_{\nu(\mathrm{P-H})}|$$

where $I_{\nu(\mathrm{P-H})}$ and $I^{\mathrm{Max}}_{\nu(\mathrm{P-H})}$ are the heights of the given P–H band and the most intense P–H band, respectively. A comparison of the theory to experiment reveals that good agreement has been achieved in most cases. Datively bonded PH_3 adsorbed onto an In–P heterodimer (cluster **2**) is predicted to yield symmetric and asymmetric stretching modes at 2318 and 2338 cm^{-1}, respectively. These modes correspond to the experimentally observed peaks at 2319 and 2339 cm^{-1}. Dissociative adsorption of PH_3 on the In-P heterodimer (cluster **3**) generates P–H and PH_2 species. The cluster calculations predict a stretching vibration at 2319 cm^{-1} for the isolated P–H bond, and at 2245 and 2255 cm^{-1} for the symmetric and asymmetric stretching modes of the PH_2 group. The last two modes most likely correspond to the experimental infrared peaks at 2242, and 2262 cm^{-1}, respectively. The isolated P–H mode calculated at 2319 cm^{-1} is tentatively assigned to the experimental peak at 2301 cm^{-1} (*vide infra*).

Cluster **4** exhibits symmetric and asymmetric stretching modes for PH_3 datively bonded to the In–In dimer at 2296 and 2329 cm^{-1}, respectively. The corresponding peaks observed by experiment occur at 2285 and 2327 cm^{-1}. Dissociative adsorption of phosphine at this site results in a PH_2 group and bridging indium hydride as illustrated by cluster **5**. According to the theory, the symmetric and asymmetric stretching modes of the PH_2 groups are at 2233 and 2242 cm^{-1}, whereas the experiment yields frequencies of 2226 and 2242 cm^{-1}, respectively.

Although the theory predicts the symmetric and asymmetric stretching modes of PH_3 and PH_2 species on the surface very well within a difference of a few wavenumbers, it predicts the isolated P–H stretching mode on the adatom dimer with a difference of 18 cm^{-1}. This is clearly an artifact of our present cluster model, since it does not include the effect of the In–In dimers on the *other side* of the In–P adatom dimer. More detailed calculations are needed with larger cluster models to assign this mode more definitively. The 2219 cm^{-1} frequency mode has not been assigned thus far. While it is close enough to the 2226 cm^{-1} mode to be assigned to the symmetric stretch of a PH_2 group, its low frequency may also be due to a longer P–H bond associated with the presence of a lone pair on the phosphorus atom. It should be noted that a similar stretching mode has been observed previously in the case of hydrogen adsorption on the P-rich InP surface [15].

The assignment of the peaks at 2319 and 2285 cm^{-1} to the symmetric stretching modes of datively bonded PH_3 and TBP is further supported by the annealing experiments. Since this bond is weak, the molecule should desorb at a relatively low temperature. As seen in the difference spectrum in Fig. 3, the intensities of the peaks at 2285 and 2319 cm^{-1} decrease significantly more than the other P–H peaks as the temperature is raised from 25 to 180 °C.

4.2. Adsorption sites

The adsorption mechanism proposed by Sun et al. [13], reactions (1)–(3) in the Introduction, is consistent with the results obtained in the present study. Shown in Fig. 8 is a potential energy diagram for phosphine adsorption, obtained from molecular cluster calculations [26]. In reaction (1), the group V precursor makes a dative bond to the empty dangling orbital of the indium atom with a binding energy of −11 kcal/mol. In reaction (2), the molecule dissociates into adsorbed PH_2 by transferring hydrogen or a *t*-butyl ligand to a nearby phosphorus adsorption site. According to the theory, this reaction requires activation energy of 17 kcal/mol. In order to conserve electrons, the PH_2 group will have a lone pair of electrons attached to the P atom. This gives rise to the stretching modes at 2242 and 2262 cm^{-1}. The cluster calculations further predict that dissociation of the PH_2 species is not possible at room temperature. The reader is referred to Ref. [26] for a detailed discussion of the reaction mechanism.

During the dissociative adsorption of PH_3 on the In–In dimer, the hydrogen ligand is predicted to insert into the indium bridge bond. However, here the calculated activation energy is 30 kcal/mol [26]. This energy barrier is too high for the reaction to occur at room temperature. However, vibrational modes ascribable to PH_2 bound to the In–In dimer are observed experimentally, i.e., at 2219 (2212) and 2226 cm^{-1}. Surface diffusion of the PH_2 species from the In-P heterodimer to the In–In dimer could explain this result, as this process would have a much lower energy barrier. Similarly, hydrogen atoms may diffuse from

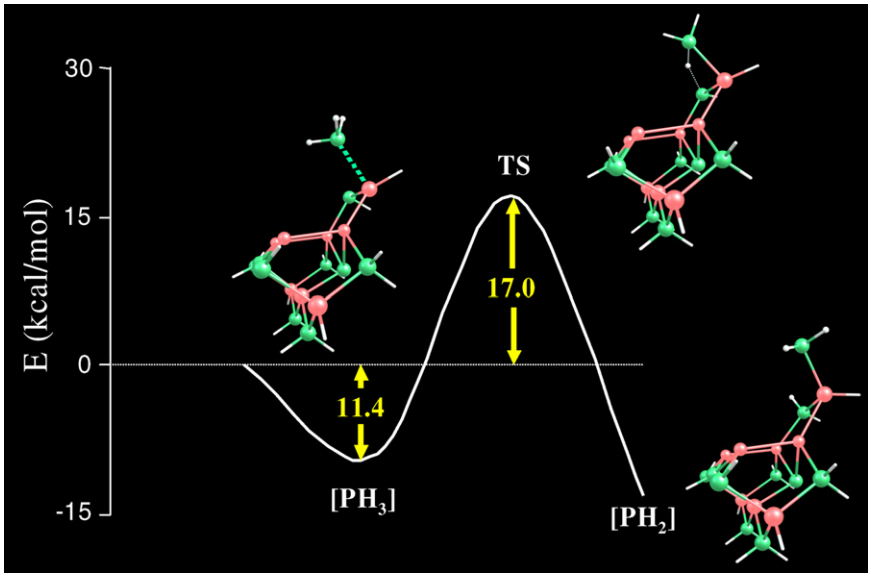

Fig. 8. Potential energy diagram for phosphine adsorption and dissociation into PH_2.

phosphorus adsorption sites to In–In bridging sites and produce indium hydrides band with vibrational frequencies between 1750 and 1000 cm^{-1}. These bands can be observed in the infrared spectra presented in Fig. 1.

Listed in Table 1 are the estimated percentages of P and In atoms observed by XPS following phosphine and tertiarybutylphosphine adsorption on InP (001). A comparison of the P/In ratio indicates that the saturation coverage of PH_3 is higher than that of TBP. The calculated van der Waals diameters from the critical pressures and temperatures for PH_3 and TBP are 4.41 and 6.01 Å, respectively [23,25]. With a fixed InP unit cell dimension of 4.0×4.0 $Å^2$ for the (1×1), more phosphine molecules should be able to adsorb than TBP molecules, as observed. Nevertheless, we do not believe that the phosphorus coverage is truly 2.2 for phosphine adsorbed on the InP (001)-(2×4) surface. Since the number of photoelectrons detected by XPS decreases exponentially with depth, the datively bonded phosphine molecules protruding out of the surface would tend to over-emphasize the abundance of these species relative to P and In in the lower layers. For example, with an escape depth of 12 Å, photoelectrons from the 4 top most P layers and the 4 top most In layers of the (2×1) surface will be detected by XPS. By contrast, for the phosphine covered (2×4) surface, photoelectrons from the 4 top most P layers and 3 top most In layers will be detected.

The infrared study presented here provides solid evidence for the formation of datively bonded phosphine and tertiarybutylphosphine on InP (001). This reaction is reversible with molecular desorption increasing rapidly with surface temperature. At the same time, a portion of the adsorbed PH_3 and TBP undergo dissociative adsorption on the In–P heterodimer. Molecular desorption competes effectively with sequential dissociation adsorption, so that at elevated temperatures the sticking probability of the group V molecules is low, i.e., between 0.001 and 0.007 [13,14]. The calculated binding energy of TBP on the indium phosphide surface is about 3–4 kcal/mol higher than that of PH_3, consistent with the slightly higher sticking probability of TBP.

5. Conclusions

We have characterized the adsorption of phosphine and tertiarybutylphosphine on the indium-rich InP (001)-(2×4) surface by vibrational spectroscopy, X-ray photoemission, and low-energy electron diffraction. The group V molecules first form dative bonds to exposed indium atoms on the surface, and then undergo dissociation into PH_2, with transfer of the H or tertiarybutyl ligands to adjacent phosphorus sites. The weakly held molecular state provides an explanation for the low sticking probability of PH_3 and TBP under MOCVD growth conditions.

Acknowledgements

Funding for this research was provided by Spectrolab, Inc. (a division of Boeing), Epichem, Inc., SAES Getters, Inc., and the UC Discovery program. K. Raghavachari and U. Das acknowledge support from American Chemical Society, Petroleum Research Fund grant (PRF 43465-AC10).

References

[1] H.-G. Bach, W. Schlaak, G.G. Mekonnen, A. Seeger, R. Steingruber, C. Schramm, G. Jacumeit, R. Ziegler, A. Umbach, G. Unterborsch, W. Passenberg, W. Ebert, T. Eckardt, in: Trends in Optics and Photonics, Optical Fiber Communication Conference, vol. 37, Baltimore, MD, USA, 2000.

[2] F. Alexandre, J.L. Benchimol, J. Dangla, C. Dubon-Chevallier, V. Amarger, Electron. Lett. 26 (1990) 1753.
[3] M.T. Camargo Silva, J.E. Zucker, L.R. Carrion, C.H. Joyner, A.G. Dentai, IEEE J. Sel. Top. Quant. 6 (2000) 26.
[4] Y. Akage, K. Kawano, S. Oku, R. Iga, H. Okamoto, Y. Miyamoto, H. Takeuchi, Electron Lett. 37 (2001) 299.
[5] G.B. Stringfellow, Organometallic Vapor-Phase Epitaxy: Theory and Practice, Academic press, San Diego, 1989.
[6] <http://www.compoundsemiconductor. net/articles/magazine/8/1/6/1>.
[7] S.D. Adamson, B.-K. Han, R.F. Hicks, Appl. Phys. Lett. 69 (1996) 3236.
[8] G. Miller, Solid State Technol. 32 (1989) 59.
[9] K.L. Hess, R.J. Riccio, J. Crystal Growth 77 (1986) 95.
[10] G. Chen, D. Cheng, R.F. Hicks, A.M. Noori, S.L. Hayashi, M.S. Goorsky, R. Kanjolia, R. Odedra, J. Crystal Growth 270 (2004) 322.
[11] M.J. Begarney, C.H. Li, D.C. Law, S.B. Visbeck, Y. Sun, R.F. Hicks, Appl. Phys. Lett. 78 (2001) 55.
[12] G. Kaneda, N. Sanada, Y. Fukuda, Appl. Surf. Sci. 142 (1999) 1.
[13] Y. Sun, D.C. Law, S.B. Visbeck, R.F. Hicks, Surf. Sci. 513 (2002) 256.
[14] Y. Sun, D.C. Law, R.F. Hicks, Surf. Sci. 540 (2003) 12.
[15] Q. Fu, E. Negro, G. Chen, D.C. Law, C.H. Li, R.F. Hicks, K. Raghavachari, Phys. Rev. B 65 (2002) 075318.
[16] L. Li, Q. Fu, C.H. Li, B.-K. Han, R.F. Hicks, Phys. Rev. B 61 (15) (2000) 10223.
[17] W.G. Schmidt, Phys. Rev. B 57 (1998) 14596.
[18] K. Raghavachari, Q. Fu, G. Chen, L. Li, C.H. Li, D.C. Law, R.F. Hicks, J. Am. Chem. Soc. 124 (2002) 15119.
[19] G. Chen, S.F. Cheng, D.J. Tobin, L. Li, K. Raghavachari, R.F. Hicks, Physical Review B, Rapid Comm. 68 (2003) 121303 (R).
[20] G. Socrates, Infrared Characteristic Group Frequencies, second ed., Wiley, Chichester, England, 1994.
[21] M. Sugiyama, K. Kusunoki, Y. Shimogaki, S. Sudo, Y. Nakano, H. Nagamoto, K. Sugawara, K. Tada, H. Komiyama, Appl. Surf. Sci. 117/118 (1997) 746.
[22] G.H. Fan, R.D. Hoare, M.E. Pemble, I.M. Povey, A.G. Taylor, J. Crystal Growth 124 (1992) 49.
[23] <http://webbook.nist.gov/chemistry/>.
[24] C.H. Li, L. Li, D.C. Law, S.B. Visbeck, R.F. Hicks, Phys. Rev. B 65 (2002) 205322.
[25] D.A. McQuarrie, J.D. Simon, Physical Chemistry: A Molecular Approach, University Science Books, Sausalito, 1997.
[26] U. Das, R.L. Woo, R.F. Hicks, K. Raghavachari, in preparation.